

# ADEN ALOS PALSAR PRODUCT VERIFICATION

P.A. Wright <sup>(1)</sup>, P.J. Meadows <sup>(1)</sup>, G. Mack <sup>(2)</sup>, N. Miranda <sup>(3)</sup>, M. Lavallo <sup>(4)</sup>

<sup>(1)</sup> BAE SYSTEMS Advanced Technology Centre, West Hanningfield Road,  
Chelmsford, Essex, CM2 8HN, United Kingdom  
Email: patrica.wright@baesystems.com, peter.meadows@baesystems.com

<sup>(2)</sup> VEGA Group PLC, 2 Falcon Way, Shire Park, Welwyn Garden City,  
Hertfordshire, AL7 1TW, United Kingdom  
Email: gordon.mack@vega.co.uk

<sup>(3)</sup> European Space Agency, Directorate of Earth Observation Programmes,  
ESA-ESRIN, Via Galileo Galilei 00044, Frascati, Italy  
Email: nuno.miranda@esa.int

<sup>(4)</sup> Computer System and Production Engineering Department,  
Tor Vergata University, via del Politecnico, 1, 00133 Rome, Italy.  
Email: lavallo@disp.uniroma2.it

## ABSTRACT

Within the ALOS Data European Node (ADEN) the verification of PALSAR products is an important and continuing activity, to ensure data utility for the users.

The paper will give a summary of the verification activities, the status of the ADEN PALSAR processor and the current quality issues that are important for users of ADEN PALSAR data.

## 1. INTRODUCTION

The monitoring of PALSAR data is performed for ESA-ESRIN by the Instrument Data Quality Evaluation and Analysis Service (IDEAS). The PALSAR activities are conducted within the SAR group which possesses extensive experience of dealing with operational SAR data.

The types of activities performed using PALSAR data include the monitoring of a selection of product header parameters such as the Doppler centroid frequency; product visual inspection; impulse response function analysis (e.g. for spatial resolution measurement) using suitable point targets such as ground receiving stations; noise equivalent radar cross-section measurement; radiometric resolution and equivalent number of looks assessment; elevation antenna pattern monitoring using the African rainforest; azimuth and range ambiguities; dual and quad polarisation calibration assessment including channel coherence, balance and SNR, cross-talk analysis and Faraday rotation analysis.

## 2. ROUTINE ANALYSIS

A key component of the PALSAR product verification is the routine inspection of all data products that are distributed electronically by ADEN. This forms the basis of an ongoing monitoring of product quality and also supports further, more in depth, investigations.

All PALSAR products are routinely analysed and the results of this analysis ingested into a database containing all past quality reports. These quality reports contain selected information from the PALSAR headers which is continually compared to the baseline performance in order to highlight any product which varies from this. An example of this type of analysis which shows products exhibiting unusual Doppler frequencies due to suspension of yaw steering on ALOS is given in Figure 1 (data points at nearly -1600Hz).

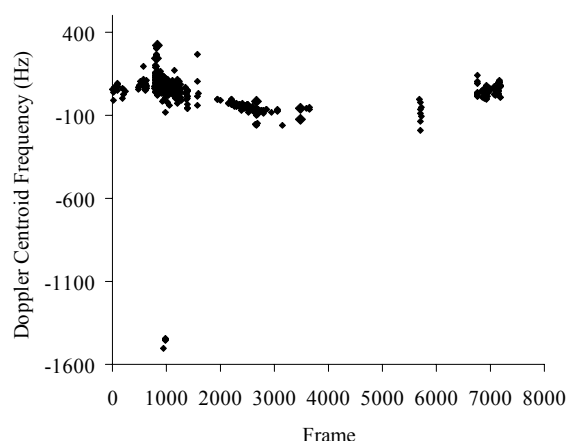


Figure 1. The Doppler centroid frequency is plotted against frame for a sample of PALSAR products.

### 3. PRODUCT VISUALISATION

Detailed visual inspections are conducted on a sample of PALSAR products, selected at random from those available. Several visual anomalies have been identified to date, the wide swath mode being particularly affected.

Some examples of typical problems observed are given in the following figures. Figure 2 shows interference effects, Figure 3 gives an example of range ambiguities which are commonly observed at the extreme near and far ranges of both wide swath and fine mode products. Figure 4 gives an example of sub swath azimuth intensity fluctuations and sub swath boundaries which are frequently present in wide swath products. Unless otherwise stated, these examples are taken from data processed with version 4.03 of the JAXA PALSAR processor.

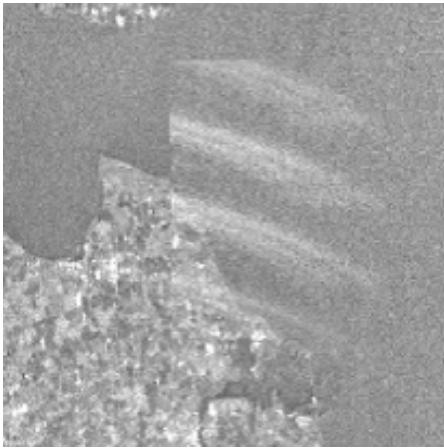


Figure 2. An example of interference effects, observed in the wide swath mode product taken from frame 2500 of orbit 4454.

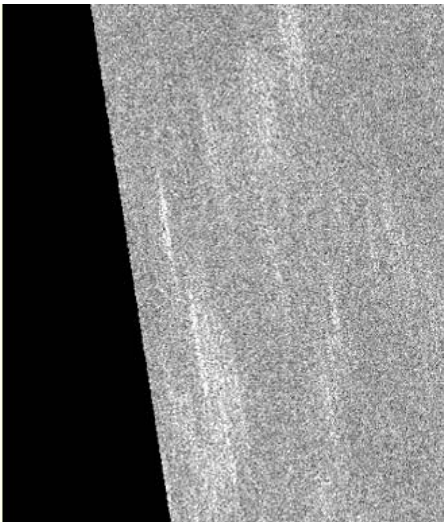


Figure 3. An example of range ambiguities taken from the near side of the fine mode product from frame 830 of orbit 5161.

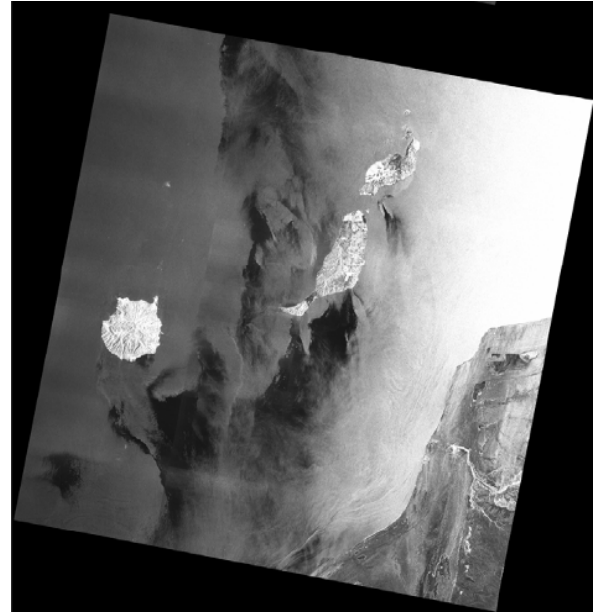


Figure 4. An example of sub swath boundaries and azimuth intensity fluctuations. This wide swath image is taken from frame 3050 of orbit 6526 and was processed with version 5.02 of the JAXA PALSAR processor.

A summary of the main anomalies found in the detailed visual inspections as of 20th October 2008 is presented in Table 1 (P refers to high resolution quad-polarisation products, W to low resolution wide swath products, H to high resolution single or dual polarisation products, 1.1 to Level 1.1 complex product and 1.5 to Level 1.5 detected products).

Product Type	P1.1	P1.5	W1.5	H1.1	H1.5
Sub-Swath Boundaries	0	0	20	0	0
Azimuth Ambiguity	0	1	7	0	5
Scalloping	0	0	10	0	1
Incorrect Antenna Pattern Correction	0	0	1	1	0
Range Ambiguity	1	2	6	5	12
Azimuth Focusing	0	0	0	1	1
Sub-Swath Range Intensity Fluctuation	0	0	3	0	0
Azimuth Intensity Fluctuation	0	0	7	0	0
Interference	0	0	6	1	0
<b>Total Number Of Products Inspected</b>	<b>19</b>	<b>28</b>	<b>46</b>	<b>34</b>	<b>68</b>

Table 1. A summary of the key visual anomalies observed during the PALSAR visual inspections. Anomalies that are no longer observed due to processor updates (e.g. the far range radiometric correction error which was removed with version 4.02 of the processor) are not reported.

#### 4. IRF ANALYSIS

PALSAR products acquired over ground stations at Maspalomas, Spain, Matera, Italy and Tromsø, Norway and the DLR corner reflectors, Germany have been used for impulse response function (IRF) analysis.

##### 4.1. Maspalomas – Wide Swath Analysis

The ESA receiving antenna at Maspalomas has been used for IRF analysis of wide swath mode data (the ground station IRF is too bright in fine mode data). Figure 5 show the resampled region around the Maspalomas ground station and slices through the IRF. The IRF measurements are given in Table 2: the incidence angle of the ground station, azimuth and range spatial resolutions, integrated sidelobe ratio (ISLR), peak sidelobe ratio (PSLR) and spurious sidelobe ratio (SSLR).

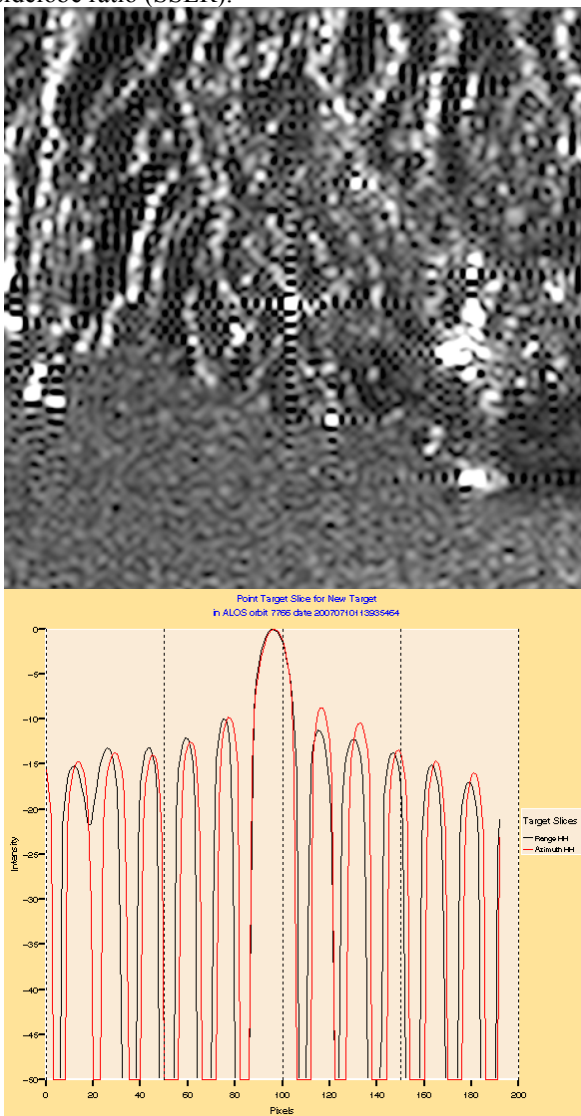


Figure 5. Wide swath image of the Maspalomas ground station (top) acquired on 10th July 2007 (orbit 7766, frame 3050) and slices through the ground station IRF.

Acq Date	Inc Ang	Azi Res (m)	Range Res (m)	ISLR (dB)	PSLR (dB)	SSLR (dB)
16/04/07	39.2	169.1	120.9	-15.1	-8.5	-11.9
10/07/07	20.2	131.7	135.3	0.5	-8.9	-9.0
25/08/07	40.7	166.8	187.6	-5.0	-10.9	-12.1
10/10/07	40.7	128.5	129.4	-7.7	-8.6	-11.5
25/11/07	40.8	165.7	123.0	-12.4	-6.5	-11.7
02/12/07	23.0	170.3	121.3	-0.9	-9.1	-9.0
11/04/08	40.8	165.3	147.5	-2.6	-11.2	-9.6
03/09/08	22.7	133.5	125.8	6.3	-4.6	-6.4

Table 2. Maspalomas WS HH IRF Measurements

The variability in the azimuth and range spatial resolutions is due to the undersampling of the wide swath imagery (adequately sampled data has the pixel size equal to half the spatial resolution – WS imagery has 100m pixels). It can also be seen that the ISLR is quite variable while the PSLR and SSLR are acceptable for this type of data.

##### 4.2. Matera – Fine Mode Analysis

The Matera ground station complex is shown in Figure 6(a). The receiving antenna is to the right of the main complex – it is not saturated in either the single or dual polarisation fine mode imagery. Figure 6(b) shows a resampled image around the receiving antenna and slices through the IRF from Level 1.1 data.

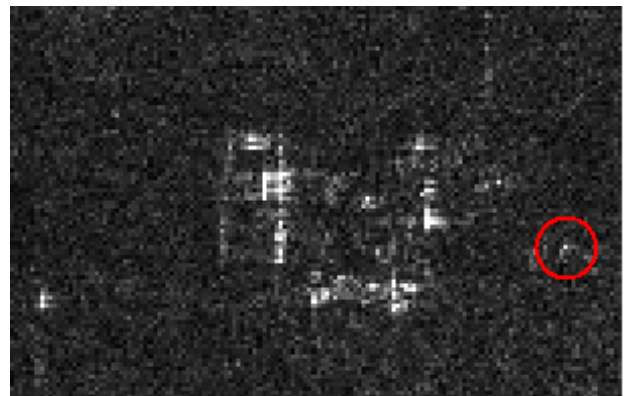


Figure 6(a). Matera ground station from a Level 1.1 fine mode single polarisation (HH) image acquired on 20th February 2007 (orbit 5730, frame 800). The ground station is to the right centre of the image (circled).

Table 3 give the IRF measurements for Level 1.5 FBS and FBD imagery (HH polarisation). Note that for the data to be adequately sampled in Level 1.5 products, the pixel size should be half the spatial resolution – the FBS pixel size is 6.25m while the FBD pixel size is 12.5m). Consequently both the FBS and FBD Level 1.5 data is

undersampled. The FBS sidelobe measurements are all quite high compared to theoretical and expected values.

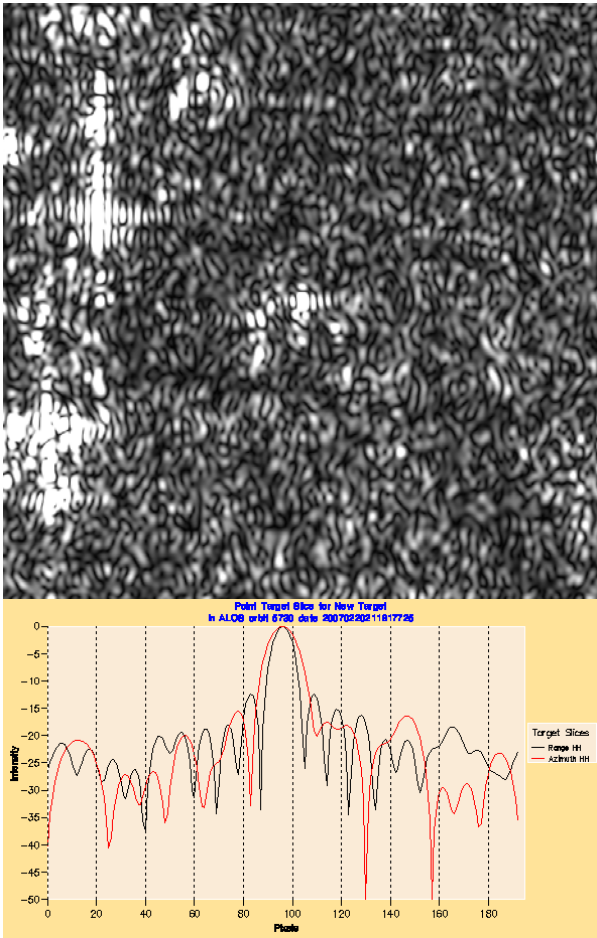


Figure 6(b). Resampled image (top) and IRF slices (bottom) for the Matera ground station from 20th February 2007 (HH polarisation)

Table 4 gives the IRF measurements for Level 1.1 HH polarisation data (adequately sampled). Note that the range resolution is the slant range resolution and that this and the azimuth resolution values are quite consistent from image to image. They are also comparable with their theoretical values. However, the ISLR values are quite high compared to theoretical and expected values – this is probably due to the radar cross-section of the ground station is quite low ( $\sim 30\text{dBm}^2$ ) and consequently the background is quite high in relation to the ground station IRF. This is also why the Level 1.1 PSLR and SSLR values are not calculated.

Acq Date	Inc Ang	Azi Res (m)	Range Res (m)	ISLR (dB)	PSLR (dB)	SSLR (dB)
20/02/07	38.7	8.5	7.7	-9.4	-7.9	-10.7

Table 3(a). Matera FBS Level 1.5 IRF Measurements

Acq Date	Inc Ang	Azi Res (m)	Range Res (m)	ISLR (dB)	PSLR (dB)	SSLR (dB)
23/08/07	38.6	21.2	21.2	11.5	-0.8	10.9

Table 3(b). Matera FBS Level 1.5 IRF Measurements

Acq Date	Inc Ang	Azi Res (m)	Range Res (m)	ISLR (dB)	PSLR (dB)	SSLR (dB)
05/01/07	38.9	4.47	4.59	-3.47	-	-
20/02/07	38.8	4.47	4.47	-2.10	-	-
08/01/08	38.7	4.59	4.61	-3.78	-	-
23/02/08	38.6	4.28	4.55	-1.34	-	-
09/04/08	38.6	4.23	4.44	-0.00	-	-

Table 4(a). Matera FBS Level 1.1 IRF Measurements

Acq Date	Inc Ang	Azi Res (m)	Range Res (m)	ISLR (dB)	PSLR (dB)	SSLR (dB)
08/07/07	38.7	4.75	9.33	0.93	-	-
23/08/07	38.7	4.61	9.20	1.15	-	-
25/05/08	38.6	5.71	9.56	1.79	-	-
10/07/08	38.8	4.37	10.00	2.61	-	-
25/08/08	38.9	4.71	9.08	4.79	-	-
25/08/08	38.9	5.46	9.91	2.68	-	-

Table 4(b). Matera FBS Level 1.1 IRF Measurements

### 4.3. Tromsø – Fine Mode Analysis

The Tromsø ground station is shown in Figure 7(a). The receiving antenna is not saturated in either the single or dual polarisation fine mode imagery. Figure 7(b) shows a resampled image around the receiving antenna and slices through the IRF from Level 1.1 data.

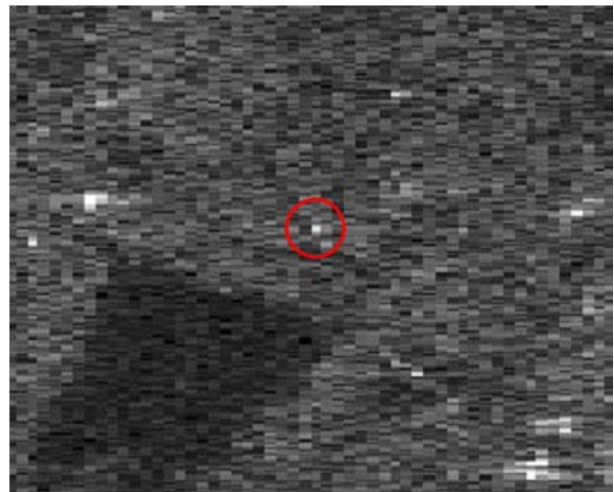


Figure 7(a). Tromsø ground station from a Level 1.1 fine mode dual polarisation (HH) image acquired on 2nd October 2007 (orbit 8997, frame 1390). The ground station is to the middle of the image (circled).

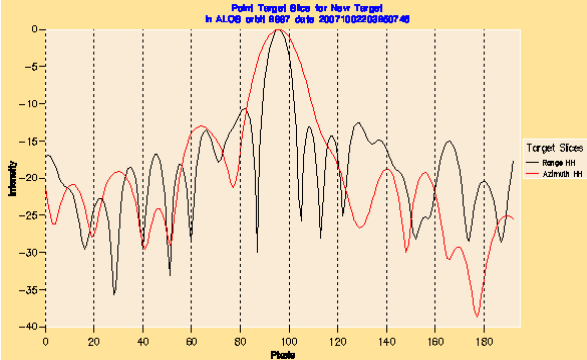
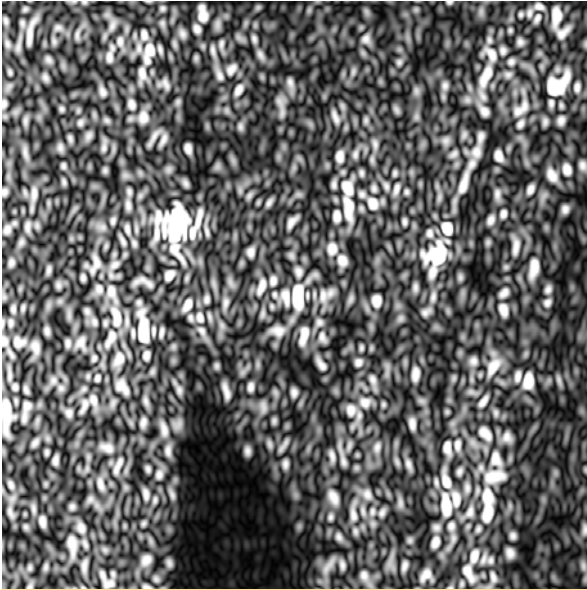


Figure 7(b). Resampled image (top) and IRF slices (bottom) for the Tromsø ground station from 2nd October 2007 (HH polarisation)

Table 5 give the IRF measurements for Level 1.5 FBS and FBD imagery (HH polarisation). The spatial resolution measurements indicate that both the FBS and FBD Level 1.5 data is undersampled. The sidelobe measurements are all quite high compared to theoretical and expected values.

Table 6 gives the IRF measurements for Level 1.1 HH polarisation data (adequately sampled). The spatial resolution measurements are comparable with their theoretical values. However, the ISLR values are quite high – this is probably due to the radar cross-section of the ground station is quite low ( $\sim 30\text{dbm}^2$ ) and consequently the background is quite high in relation to the ground station IRF. This is also why the Level 1.1 PSLR and SSLR values are not calculated.

Acq Date	Inc Ang	Azi Res (m)	Range Res (m)	ISLR (dB)	PSLR (dB)	SSLR (dB)
11/01/07	37.6	12.0	7.9	1.57	-2.59	-6.21

Table 5(a). Tromsø FBS Level 1.5 IRF Measurements

Acq Date	Inc Ang	Azi Res (m)	Range Res (m)	ISLR (dB)	PSLR (dB)	SSLR (dB)
02/07/07	39.9	15.7	16.1	8.18	-6.34	-9.10
02/10/07	39.8	18.0	15.4	8.67	-6.58	-3.02
19/05/08	39.6	17.9	18.0	3.05	-4.04	-6.20
19/08/08	40.2	17.4	20.7	7.91	-7.48	-6.52

Table 5(b). Tromsø FBD Level 1.5 IRF Measurements

Acq Date	Inc Ang	Azi Res (m)	Range Res (m)	ISLR (dB)	PSLR (dB)	SSLR (dB)
11/01/07	37.6	7.54	4.11	-3.08	-	-
14/02/07	40.0	4.61	4.68	1.53	-	-

Table 6(a). Tromsø FBS Level 1.1 IRF Measurements

Acq Date	Inc Ang	Azi Res (m)	Range Res (m)	ISLR (dB)	PSLR (dB)	SSLR (dB)
02/07/07	40.0	5.29	9.70	5.79	-	-
14/07/07	37.5	6.31	9.00	10.28	-	-
17/08/07	39.9	4.54	9.80	8.79	-	-
02/10/07	39.9	5.86	9.28	5.40	-	-

Table 6(b). Tromsø FBD Level 1.1 IRF Measurements

#### 4.4. DLR Corner Reflectors – Fine Mode Analysis

During the ADEN commissioning phase six corner reflectors deployed by DLR, Germany [1] as suitable point targets for IRF analysis. The average IRF measurements for the six DLR corner reflectors from quad-polarimetric (PLR) Level 1.5 and 1.1 products as given in Tables 7 and 8.

The Level 1.5 spatial resolution measurements indicate that the products are undersampled in azimuth (the PLR pixel size is 12.5m) but not in range. The ISLR values are higher than expected while the PSLR and SSLR values are reasonable. Note that all the DLR corner reflectors have a few peak IRF pixels that are saturated in the product which, along with the undersampling, contributes to the properties of Level 1.5 IRFs.

Acq Date	Pol	Azi Res (m)	Range Res (m)	ISLR (m)	PSLR (m)	SSLR (m)
06/09/06	HH	16.7	22.3	-1.1	-6.0	-12.7
06/09/06	VV	16.5	26.4	-1.2	-8.4	-12.7
15/11/06	HH	18.0	27.3	-0.1	-7.7	-10.0
15/11/06	VV	17.1	26.7	0.9	-7.5	-10.6

Table 7. DLR CR PLR Level 1.5 Measurements

In the Level 1.1 products the DLR corner reflector IRFs are not saturated and the data is adequately sampled. The spatial resolution measurements are comparable with their theoretical values and the sidelobe ratios are

much lower than the corresponding Level 1.5 measurements.

Acq Date	Pol	Azi Res (m)	Range Res (m)	ISLR (m)	PSLR (m)	SSLR (m)
06/09/06	HH	4.48	9.63	-5.2	-12.7	-17.2
06/09/06	VV	4.44	9.85	-5.3	-14.0	-14.7
15/11/06	HH	4.58	9.77	-5.4	-11.6	-16.7
15/11/06	VV	4.66	9.78	-5.7	-11.2	-17.4

Table 8. DLR CR PLR Level 1.1 Measurements

## 5. RADIOMETRIC STABILITY

A successful method of assessing the stability of SAR instruments such as ERS-2 SAR and Envisat ASAR has been to use the Amazon rainforest by calculating gamma ( $\sigma^0/\cos(i)$  where  $\sigma^0$  is radar cross-section and  $i$  is incidence angle) for a given location and determining its variation over time. Since Amazon rainforest data is not available for PALSAR data within the ADEN node, an alternative site within the African rainforest has been selected (at 2.91°N, 14.32°E). Figure 8(a) shows an example of the selected PALSAR frame while Figure 8(b) shows the corresponding profile of gamma across the swath. The mean gamma for the whole scene is -5.81dB (HH polarisation) and there is a small downward trend from near to far range of 0.10dB.

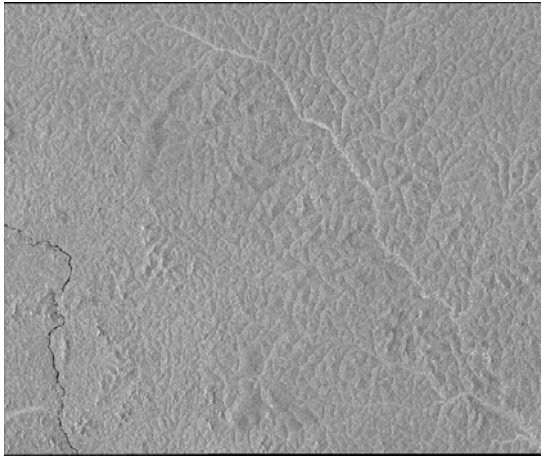


Figure 8(a). Fine Mode Level 1.5 PALSAR image of the African Rainforest from an acquisition on 9th October 2007 (orbit 9100, frame 0040, HH polarisation)

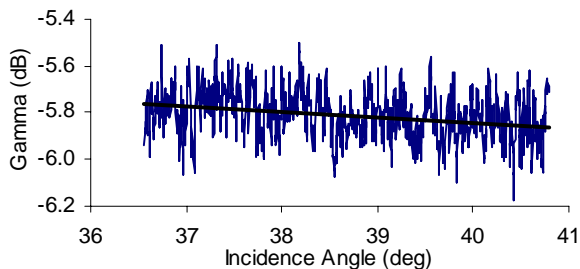


Figure 8(b). Gamma range profile from 9th October 2007

Table 9 gives the mean gamma and the trend for images acquired from the same track and frame and hence of the same region between February 2007 and April 2008. As can be seen there is some variability in the mean gamma (max – min = 0.18dB) but more importantly the shape of the gamma profile in range has changed with there being a reduction in gamma and then a rise in gamma from near to far range. The most recent image shows again no change in gamma from near to far range. The mean gamma for all 6 images is  $-5.76 \pm 0.07$  dB. This indicates an excellent radiometric stability of just 0.07dB.

Acq Date	Orbit	Mean Gamma	Trend
21/02/07	5745	-5.75 dB	-0.02 dB
09/10/07	9100	-5.81 dB	-0.10 dB
24/11/07	9771	-5.82 dB	-0.23 dB
09/01/08	10442	-5.84 dB	0.27 dB
24/02/08	11113	-5.70 dB	0.37 dB
10/04/08	11784	-5.66 dB	0.00 dB

Table 9. Mean Gamma and trend for Fine Mode African Rainforest Imagery (HH polarisation)

## 6. NOISE EQUIVALENT SIGMA ZERO

The upper limit to the noise equivalent radar cross-section (NESigma0) of an image can be estimated by measuring the radar cross-section of low intensity regions (usually ocean region under low wind speed conditions). Figure 9 shows the lowest NESigma0 measurements at each incidence angle from all product types (note there have not been any VV measurements to date). The mean NESigma0 results are given in Table 10 compare favourably with the JAXA specifications of -21dB for HH & VV polarisations and -25dB for HV & VH polarisations.

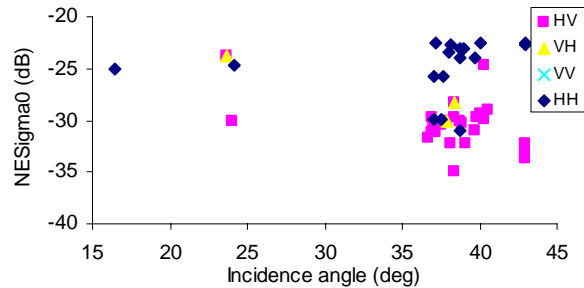


Figure 9. PALSAR NESigma0 Measurements

Polarisation	NESigma0
HH	-24.84±2.89
HV	-30.61±1.96
VH	-27.44±3.23

Table 10. Mean NESigma0

## 7. EQUIVALENT NUMBER OF LOOKS AND RADIOMETRIC RESOLUTION

The equivalent number of looks and the radiometric resolution can be measured directly from PALSAR imagery by using large uniform distributed targets. Table 11 give the measurements for the various product types (FBS is single polarisation and FBD is dual polarisation fine mode imagery). The measured ENL are close to the actual ENL used in the processing.

Product	Actual ENL	ENL	Rad Res (dB)	No. Results
P1.1	1	0.87	3.17	9
P1.5	4	4.23	1.72	4
H1.1 (FBS)	1	0.98	3.04	1
H1.5 (FBS)	2	1.28	2.79	5
H1.1 (FBD)	1	0.82	3.24	2
H1.5 (FBD)	4	3.35	1.89	6
W1.5	8	7.21	1.41	7

Table 11. ENL and RR Measurements

## 8. AMBIGUITIES

Both azimuth and range ambiguities have been found in fine and wide swath mode PALSAR imagery. Figure 3 gave an example of range ambiguities while Figure 10 gives an example of azimuth ambiguities (where ambiguities from towns and the bright radar backscatter from the mountains can be seen).

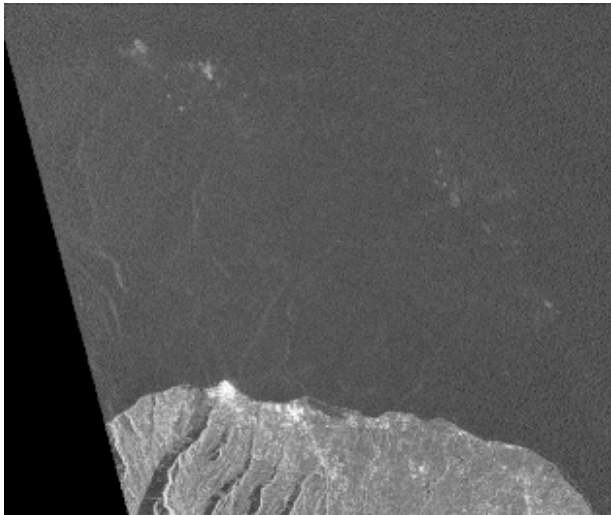


Figure 10. Azimuth ambiguities from a FBD acquisition from 20th February 2007 (orbit 5728, frame 6760)

Azimuth ambiguities of -11dB have been observed in wide swath imagery acquired on 17th May 2007 (compared to a specification of -16dB). Azimuth ambiguities have been measured up to -13.5dB in HV polarisation and up to -15.1dB in HH polarisation for FBD imagery from orbit 5728, frame 6760 (acquired

20th February 2007). FBS HH ambiguity measurements in the range -13.5dB to -14.3dB have been made for a product from orbit 11558, Frame 2800 from the 26th March 2008.

## 9. IMAGE LOCALISATION

Although the ALOS platform operates with yaw steering it does not acquire data with a non-zero Doppler. This is because the ALOS yaw axis is aligned with the centre of the earth rather than being aligned to maintain local orthogonality. A consequence of this type of yaw steering is that the Doppler frequency is not set to zero and changes as a function of latitude and beam number [2]. The ADEN PALSAR ground range Level 1.5 products are processed to zero-Doppler but the slant range Level 1.1 products are not. Consequently Level 1.1 products need to have a range dependant azimuth shift applied [3].

The absolute localisation accuracy (ALE) is the difference between the predicted and measured pixel positions of a known point target. Results using the average of the six DLR corner reflectors are shown in Tables 12 and 13 for Level 1.1 and Level 1.5 products [1]. The Level 1.1 range ALE is small at less than 6m while the azimuth ALE is still less than 20m in all but one of the products. The Level 1.5 range ALE differs between products and is up to 100m in one case. In azimuth there is less difference in the ALE at less than 20m.

Acq Date	Product Type	Range ALE (m)	Azimuth ALE (m)
06/08/06	FBS	-4.87	-18.37
01/08/06	FBS	-4.38	5.90
14/07/06	FBD	-5.16	46.25
23/05/06	FBD	-1.03	-16.90
06/09/06	PLR	-4.80	6.55
15/11/06	PLR	-1.91	4.84

Table 12. PALSAR Level 1.1 Absolute Localisation

Acq Date	Product Type	Range ALE (m)	Azimuth ALE (m)
06/08/06	FBS	30.08	-6.72
01/08/06	FBS	-0.87	-7.12
14/07/06	FBD	-103.79	6.32
23/05/06	FBD	48.57	-2.86
06/09/06	PLR	-6.38	-19.48
15/11/06	PLR	-26.78	1.02

Table 13. PALSAR Level 1.5 Absolute Localisation

## 10. POLARIMETRIC CALIBRATION

All polarimetric and Faraday measurements are performed on Level 1.1 data. The results presented here help to assess the polarimetric calibration that is applied to the data.

### 10.1. Co-registration

The quad polarisation (PLR) mean channel registration in range is  $0.94 \pm 0.80\text{m}$  and  $0.83 \pm 0.98\text{m}$  in azimuth (i.e. sub-pixel). For dual polarisation (FBD) data, the mean channel registration in range is  $1.34 \pm 1.04\text{m}$  and in azimuth is  $1.06\text{m} \pm 0.71\text{m}$  (i.e. sub-pixel).

### 10.2. Channel coherence, balance and symmetry

Parameters that may indicate problems with the data calibration are provided in Table 14.

The phase of the HVVH correlation and the HV/VH amplitude ratio are expected to have zero mean distribution. Deviations from zero mean indicate an uncompensated amplitude imbalance. The HHHV and VVVH coherence values should also be zero; if greater than 0.3 they indicate the presence of uncorrected cross talk and/or Faraday rotation. If the values are not similar, they indicate a non reciprocal cross talk. A significant HHVV mean phase deviation from zero may indicate uncorrected phase imbalance, depending on the scattering surface.

Orbit	Frame	HVVH phase Mean	HV/VH amplitude Mean (dB)	SNR Mean (dB)	VVVH coherence Mean	HHHV coherence Mean	HHVV phase Mean
4230	7150	$0.33 \pm 2.71^\circ$	$-0.27 \pm 3.47$	$11.67 \pm 1.47$	$0.09 \pm 0.05$	$0.09 \pm 0.05$	$6.58 \pm 13.59^\circ$
5650	2640	$2.11 \pm 21.11^\circ$	$0.15 \pm 5.77$	$5.31 \pm 5.69$	$0.14 \pm 0.08$	$0.15 \pm 0.09$	$-4.62 \pm 23.68^\circ$
6248	2690	$4.79 \pm 11.6^\circ$	$0.03 \pm 6.33$	$3.65 \pm 3.72$	$0.19 \pm 0.12$	$0.22 \pm 0.14$	$3.72 \pm 14.7^\circ$
6321	2640	$3.04 \pm 33.07^\circ$	$0.21 \pm 6.53$	$1.11 \pm 6.20$	$0.20 \pm 0.10$	$0.22 \pm 0.11$	$6.05 \pm 26.61^\circ$
6327	1370	$0.91 \pm 2.79^\circ$	$0.05 \pm 4.99$	$8.01 \pm 2.65$	$0.11 \pm 0.61$	$0.14 \pm 0.07$	$-2.04 \pm 5.21^\circ$
6474	1080	$26.52 \pm 22.84^\circ$	$-0.97 \pm 7.41$	$-3.31 \pm 2.59$	$0.19 \pm 0.08$	$0.19 \pm 0.07$	$4.32 \pm 7.41^\circ$
6575	1380	$1.21 \pm 2.39^\circ$	$0.09 \pm 4.77$	$9.80 \pm 2.62$	$0.12 \pm 0.06$	$0.14 \pm 0.07$	$0.02 \pm 3.90^\circ$
6940	1260	$23.06 \pm 24.55^\circ$	$3.20 \pm 5.50$	$6.14 \pm 3.82$	$0.26 \pm 0.11$	$0.23 \pm 0.11$	$19.26 \pm 9.61^\circ$
7024	800	$3.12 \pm 15.17^\circ$	$-0.09 \pm 6.66$	$1.77 \pm 4.51$	$0.21 \pm 0.11$	$0.23 \pm 0.12$	$3.94 \pm 10.71^\circ$
7072	1020	$2.17 \pm 22.64^\circ$	$-0.16 \pm 6.55$	$1.35 \pm 5.76$	$0.14 \pm 0.08$	$0.17 \pm 0.11$	$6.17 \pm 27.69^\circ$
7189	100	$24.01 \pm 2.00^\circ$	$3.35 \pm 3.96$	$11.67 \pm 1.57$	$0.10 \pm 0.05$	$0.11 \pm 0.06$	$21.01 \pm 10.61^\circ$
7233	100	$0.90 \pm 1.22^\circ$	$0.25 \pm 3.50$	$12.23 \pm 1.81$	$0.09 \pm 0.05$	$0.09 \pm 0.05$	$-1.58 \pm 14.80^\circ$
7261	100	$3.29 \pm 15.28^\circ$	$0.18 \pm 4.39$	$11.78 \pm 4.61$	$0.10 \pm 0.06$	$0.11 \pm 0.06$	$0.55 \pm 6.66^\circ$
7276	100	$1.08 \pm 1.34^\circ$	$0.05 \pm 3.64$	$11.73 \pm 2.07$	$0.09 \pm 0.05$	$0.1 \pm 0.05$	$7.14 \pm 9.55^\circ$

Table 14. PALSAR Polarimetric Coherence Measures

### 10.3. Cross talk analysis

Table 15 gives the cross talk values, where:

- A is the channel reciprocity
- W is the transmit H to V cross talk
- U is the receive H to V cross talk
- V is the transmit V to H cross talk
- Z is the receive V to H cross talk

The cross talk is calculated for polarimetric level 1.1 products only. Measures taken over specific regions are given in Table 14. In general these values are consistent with those measured by JAXA [4] and are as good as or better than the instrument specification of -30dB.



Orbit	Latitude (°)	Frame	Calculated values (mean)				
			A	U(dB)	Z(dB)	W(dB)	V(dB)
5650	48.136	2640	0.976	-33.03±0.10	-33.26±1.84	-34.77±2.82	-36.94±0.64
6321	48.137	2640	0.862	-21.19±2.38	-25.83±1.51	-23.66±0.54	-31.75±5.07
6940	62.286	1260	0.923	-29.68±0.00	-30.24±0.03	-30.81±0.10	-31.64±2.32
7072	51.077	1020	0.966	-32.69±4.98	-31.11±0.96	-35.65±2.57	-36.08±4.89
7189	5.500	100	1.19	-48.57±0.81	-34.44±0.51	-32.43±8.14	-31.25±2.53
7204	40.248	800	0.829	-26.19±8.43	-31.75±5.71	-25.29±5.76	-29.33±2.89

Table 15. Cross Talk Measurements using Selected Image Regions

Cross talk measurements have also been obtained from entire images, are shown in Table 16, and generally indicate a higher degree of cross talk than suggested by measurements from selected sites given in Table 15.

Figure 11 shows a range variation analysis of the cross-talk parameters averaged along azimuth direction over 6 PLR products. In all cases the observed values remains within the accepted values specified by JAXA.

Orbit	Latitude (°)	Frame	Calculated values (mean)				
			A	U(dB)	Z(dB)	W(dB)	V(dB)
7204	40.248	800	0.99	-25.76±6.22	-23.63±6.13	-24.34±6.01	-23.39±5.92
6474	54.004	1080	1.16	-26.98±5.79	-27.43±6.22	-27.75±6.53	-27.83±6.52
6575	68.546	1380	0.94	-28.44±5.66	-27.84±5.47	-27.98±5.5	-27.92±5.55
6327	68.053	1370	0.98	-29.95±5.57	-29.72±5.54	-29.62±5.52	-29.59±5.52
7189	5.500	100	0.75	-24.35±5.47	-24.35±5.48	-24.09±5.44	-24.23±5.45
7233	5.499	100	0.77	-25.10±5.42	-24.99±5.42	-24.99±5.42	-25.16±5.42
7261	5.495	100	0.87	-27.57±5.59	-27.54±5.62	-27.16±5.54	-27.29±5.56
7276	5.500	100	0.9	-26.44±5.45	-26.65±5.43	-25.66±5.43	-26.77±5.43
6248	45.36	2690	1.00	-25.66±6.27	-23.58±5.86	-24.88±6.12	-23.84±5.64
4230	-1.96	7150	1.24	-25.43±5.42	-25.48±5.41	-25.00±5.41	-24.87±5.42

Table 16. Cross Talk Measurements using the Entire Image

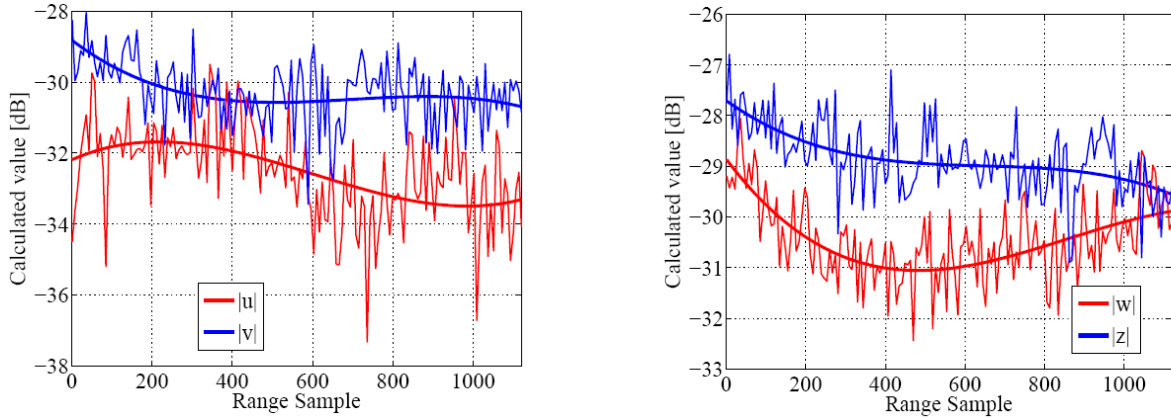


Figure 11. Cross Talk variation along range averaged over six PLR products

## 11. FARADAY ROTATION MEASUREMENTS

For any given point in the solar cycle, Faraday rotation (FR) is expected to be greatest at mid latitudes, at around 1-2pm local time, and at the equinoxes. Conversely, FR can be expected to be a minimum just

before dawn, at polar and equatorial locations and at the solstices. These generalisations can be used as a guide to assess whether the calculated FR and FR trends are plausible for a given location and time.

Faraday rotation has the effect of rotating the plane of polarisation of the transmitted and received signals. This can result in a much lower return than expected in the co-polarisation channels and a much higher return than expected in the cross-polarisation channel. This reduces the dynamic range of the co-polarised channels and drives the cross-polarised channel to resemble the co-polarised channels. This also reduces sensitivity to ground parameter variations and, for large values of FR, effectively turns a multi-polarisation radar into a single-channel system. Information products relying on the classification of L-band HV SAR data, such as crop and forest inventory or land cover maps, are likely to be affected by FR levels exceeding  $10^\circ$ . The accuracies of retrieved geophysical parameters such as soil moisture or vegetation biomass, which require good calibration and data accuracy, will be adversely affected once FR exceeds  $5\text{-}8^\circ$  (depending on land cover) [5].

FR measurements are given in Table 17 where the measured values are consistent with those expected for the time of year, day, latitude and solar activity. The measures are also within the FR tolerance; hence these images data do not need to be corrected for FR before use in geophysical retrieval. The four equatorial products (frame 100) provide a baseline mean FR value of  $0.51^\circ$ . This provides a measure of the uncertainty in the FR measurement process (the equator is unaffected by Faraday rotation). The non equatorial day time products from around the vernal equinox provide a consistent FR measure of around  $2.5^\circ$ . As we approach the next solar maximum, this level of FR will increase.

The values in Table 17 are calculated using a circular basis transformation of the full polarimetric information expressed in the H, V basis. The FR rotation can be estimated from the phase difference of the cross-polarised circular returns [6]. A second approach to estimate the FR rotation from the products takes into account the second-order statistics of the cross-polarized term in the linear basis. Finally, a third approach predicts the FR using real measurements of Total Electron Content (TEC). The three methods applied over about 30 PLR products over different areas and acquisition times have shown that the FR is always less than  $10^\circ$ . In Figure 12 it is shown the histogram of the FR estimated from PLR data products. The FR values are most concentrated around zero. Figure 13 shows the FR prediction using the TEC values and the same 30 product. In this case, most of FR values are slightly above zero but still less than  $8\text{-}10^\circ$ . Figure 14 shows the comparison between FR estimated before and after the polarimetric calibration. This analysis confirms that the polarimetric calibration has a low impact on the FR estimation (the four products below the line have processing artefacts present).

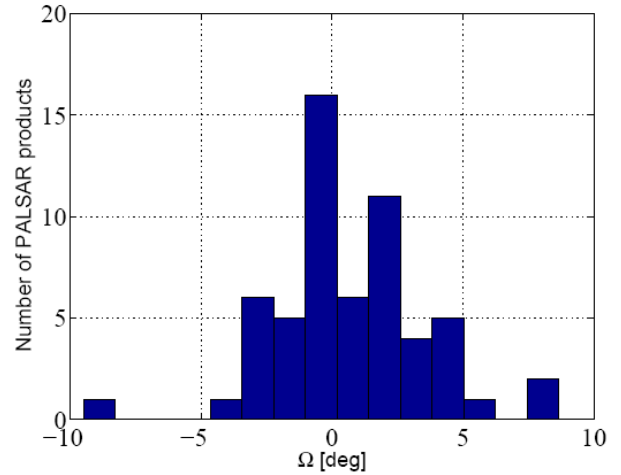


Figure 12. Histogram of the FR estimated from the PLR products using circular basis transformation

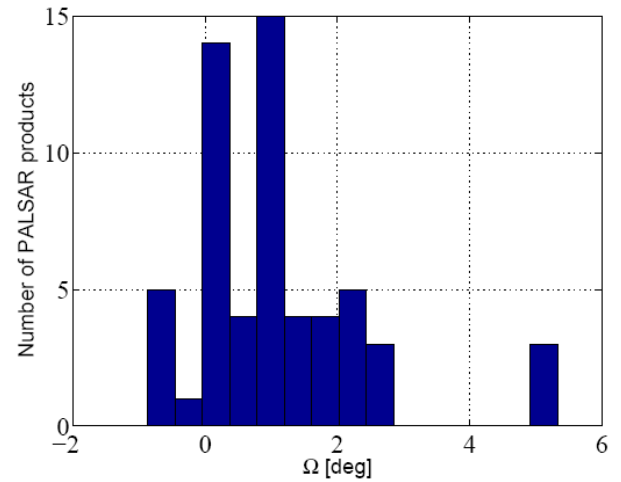


Figure 13. Histogram of FR predicted using Total Electron Content (TEC) data. The TEC data are available at CODE (<http://www.aiub.unibe.ch>.)

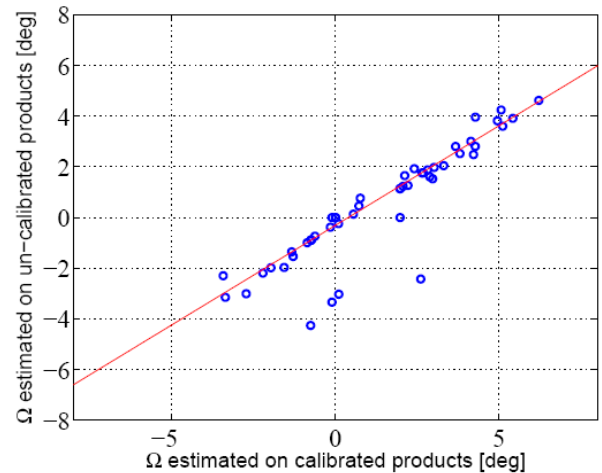


Figure 14. Comparison between FR estimated before and after the polarimetric calibration

Orbit	Latitude (deg)	Longitude (deg)	Frame	Acq. Date	UT	Local time <sup>1</sup>	Calculated FR (deg)
4230	-1.96	-61.69	7150	10/11/06	10:02	10:48	-0.98±0.21
5650	48.136	11.285	2640	15/02/07	10:05	11:06	1.13±1.03
6248	45.36	11.92	2690	28/03/07	10:00	11:06	2.50±0.34
6321	48.137	11.276	2640	02/04/07	10:06	11:06	2.54±1.14
6327	68.053	28.538	1370	02/04/07	19:41	21:18	0.90±0.18
6474	54.004	8.294	1080	12/4/07	21:28	21:50	0.76±0.24
6575	68.546	27.594	1380	19/4/07	19:43	21:05	0.95±0.17
6940	62.286	23.88	1260	14/05/07	20:13	21:26	3.02±0.34
7072	51.077	11.017	1020	23/05/07	21:21	21:50	1.20±0.53
7189	5.500	14.496	100	31/05/07	21:38	22:26	0.70±0.29
7204	40.248	-3.475	800	01/06/07	22:29	22:00	1.95±0.32
7233	5.499	8.597	100	03/06/07	22:02	22:26	0.59±0.18
7261	5.495	37.564	100	05/06/07	20:06	22:26	0.35±0.2
7276	5.500	27.374	100	06/06/07	20:47	22:26	0.41±0.16

Table 17. Calculated Faraday rotation (<sup>1</sup> calculated for 22:30 hrs ascending node crossing time and spacecraft nadir at latitude of scene)

## 12. ADEN JAXA PROCESSOR STATUS

ADEN uses the PALSAR processor provided by JAXA. Prior to the transfer to operations, the IDEAS PALSAR team performs a verification of the processor. The v4.03 of the PALSAR processor has recently been upgraded to v5.02. A verification of sample v5.02 products of the African rainforest and the Maspolomas and Tromsø ground stations was performed. An example of an improvement of v5.02 has been the revised elevation antenna pattern applied to wide swath imagery which has led to a much reduced variation of gamma ( $\sigma^0/\cos(i)$ ) across the swath, as shown in Figure 15.

Based on the verification performed, the PALSAR team recommend that v5.02 become the operation version of the ADEN JAXA PALSAR processors. This occurred at the three ADEN sites of ESRIN on 10th September 2008, Matera on 19th September 2008 and Tromsø on 18th September 2008.

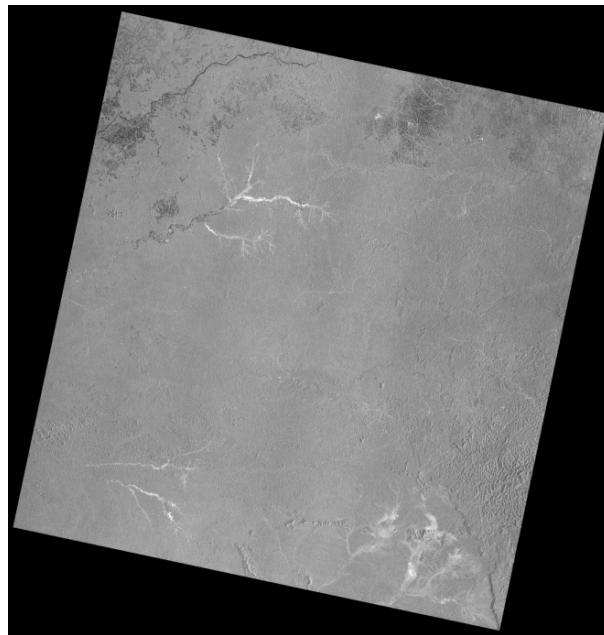


Figure 15(a). PALSAR wide swath image from 22nd June 2007 processed with v4.03

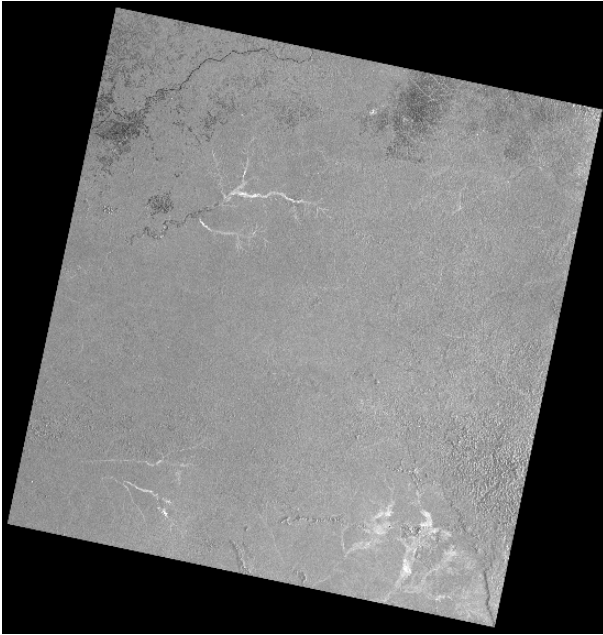


Figure 15(b). PALSAR wide swath image from 22nd June 2007 processed with v5.02 (bottom)

### 13. OTHER ISSUES AND INFORMATION

JAXA conducts PALSAR calibration acquisitions before and after normal acquisition operations. Scenes containing data from these calibration acquisitions have been found to be present in the ADEN catalogue. Processing of these products to Levels 1.1 and 1.5 will fail however it is possible to order this data at Level 1.0. An operation is currently underway to clean this data from the catalogue to avoid users ordering such data. As well as this, procedures have been put in place by the QC team to detect the distribution of affected data which may be needed in the event that the catalogue cannot be fully cleaned.

JAXA have recommended that only Level 1.1 products should be used for point target radar cross-section measurements. It should be noted that the dynamic range of Level 1.1 and Level 1.5 products is such that many point targets have pixel values at the maximum value of the 16 bit product.

ESA information about the performance of PALSAR and ADEN JAXA products can be found in [7]. This includes cyclic reports (once approved by JAXA), a FAQ, product format descriptions and processor version history. Additional information can be found at [8] including a document on PALSAR products and their radiometric calibration [9].

### 14. REFERENCES

[1] Börner, T., Papathanassiou, K.P., Marquart, N., Zink, M., Meininger, M., Meadows, P.J., Rye, A.J., Wright, P. & Rosich Tell, B., 'ALOS PALSAR

Products Verification', Proceedings of the IEEE International Geoscience and Remote Sensing Symposium, 23-27 July 2007, Barcelona, Spain.

[2] Shimada, M., Rosenqvist, A., Watanabe, M. & Tadono, T., 2005, 'The Polarimetric and Interferometric Potential of ALOS PALSAR', Proceedings of the ESA 2005 Polinsar Workshop (<http://earth.esa.int/workshops/polinsar2005/>).

[3] ADEN SAR Team, 'ALOS PALSAR Frequently Asked Questions', 2008, ALOS-PALSAR-FAQ-001 v1.1 (<http://earth.esa.int/pcs/palsar/userinfo/>).

[4] Shimada, M., 'PALSAR CALVAL Summary and Update 2007', Proceedings of the IEEE International Geoscience and Remote Sensing Symposium, 23-27 July 2007, Barcelona, Spain.

[5] Wright, P., Quegan, S., Wheadon, N. & Hall D., 'Faraday Rotation Effects on L-band Spaceborne SAR Data', IEEE Trans on Geoscience and Remote Sensing, vol. 41, 12, 2003.

[6] Freeman, A., 'Calibration of Linearly Polarized Polarimetric SAR Data Subject to Faraday Rotation', IEEE Transactions on Geoscience and Remote Sensing, vol. 42, 8, 1617–1624, 2004.

[7] ESA, Product Control Service, <http://earth.esa.int/pcs/alos/palsar/>.

[8] ESA, Earthnet Online, <http://earth.esa.int/ALOS/>.

[9] ESA, 'Information on ALOS PALSAR Products for ADEN Users', ALOS-GSEG-EOPG-TN-07-0001.